CHRONOLOGY OF DRY LAND SEDIMENTS

Fluvial Sequences

Sabarmati Basin

A 40 m thick sequence is exposed at Mahudi. The upper 7.5 m section that overlies the red soil comprises the upper fluvial sequence. This is succeeded by 1.5 m thick aeolian sand. Two such sections designated as Mahudi-A and B and exposed along the western cliffy river bank, have been studied. Mahudi-B is located 5 km inland from the present day river course (Fig. 3.1). In addition to this the younger fluvial record that was deposited after the river occupied the present course is preserved in scroll plains and is located on the left flank along the meandering loop of the Sabarmati River at Mahudi (Fig. 3.2).

A 7 5 m of greyish yellow fine sand and silt overlies the red soil with an erosional contact (Fig. 3.1). The lower 3.5 m of the unit contains laterally persistent 5-10 cm thick-bedded calcrete, which occurs, at regular intervals At some places sediment in the vicinity of calcrete beds have preserved the ripple morphology and the faint parallel laminations. Bedded calcrete become less persistent towards the upper part of this horizon where they are replaced by the nodular carbonate concretions.

Grain size analysis of the lower 3.5m indicates the dominance of very fine sand (85%)

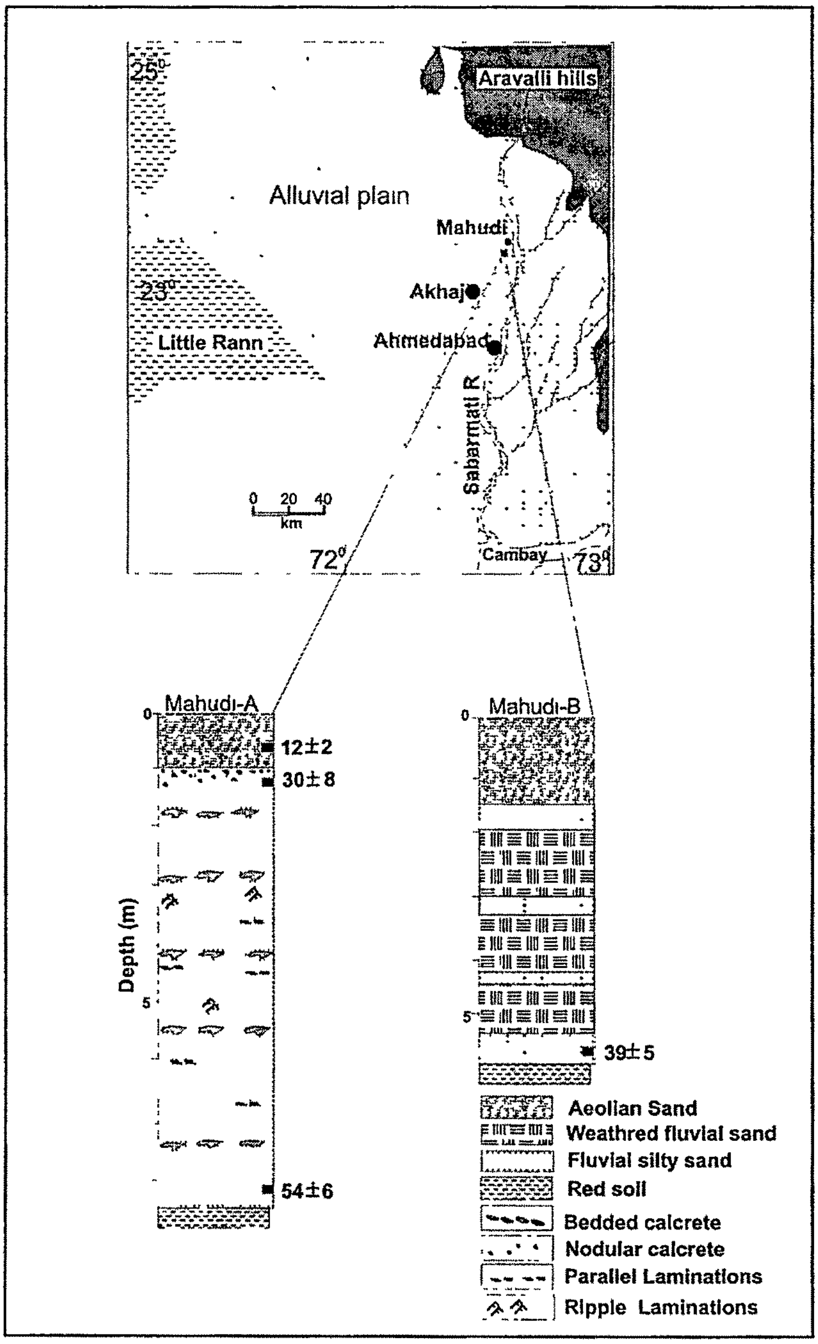

Figure-3.1. Stratigraphy and luminescence chronology of upper fluvial and aeolian sequence at Mahudi.

with silt+clay making up only 15%. The average grain size is dominated by very fine sand (3.27 ϕ) which is moderately sorted and finely skewed. Evidence of mottling is seen especially in the vicinity of bedded calcretes and root casts. The upper 4.0 m of this unit is reddish brown with a high concentration of dispersed nodular calcrete. Grain size data shows equal amounts of very fine sand and silt+clay. Compared to the underlying material, this section is rich in silt+clay and the carbonate nodules do not show any preferred horizonation. Occasional clay illuviation is seen along the moderately developed ped faces.

Scroll Plains

These are present in the modern river channel and are the direct manifestation of the deposition by the Sabarmati River (Fig 3.2A and B). Three generations of scroll plains are delineated, numbered I (oldest) to III (youngest) and are located 6 m above the present river bed (Fig. 3.2B). Scroll plain-I is currently under cultivation. This is the most extensive scroll plain being nearly 1 km wide, and bounded in the east by a subdued cliffy margin. Scroll plain-II is 500 m wide and is adjacent to the older scroll plain with an offset of 2.5 m. The youngest scroll plain-III is 3 m lower than number II and lies adjacent to the present day river channel (Fig. 3.2C). A 2.5m deep trench at the youngest edge of the scroll plain-I was excavated. From base upward the sediments show trough and planar cross stratification, overlain by 60 cm parallel laminated fine sand, and are capped by 10 cm of silty clayey sediments. Finally there is a layer of cross-bedded fine sand. The sediments are dominated by fine to medium sand (average 2.28 ϕ) and are moderately well sorted.

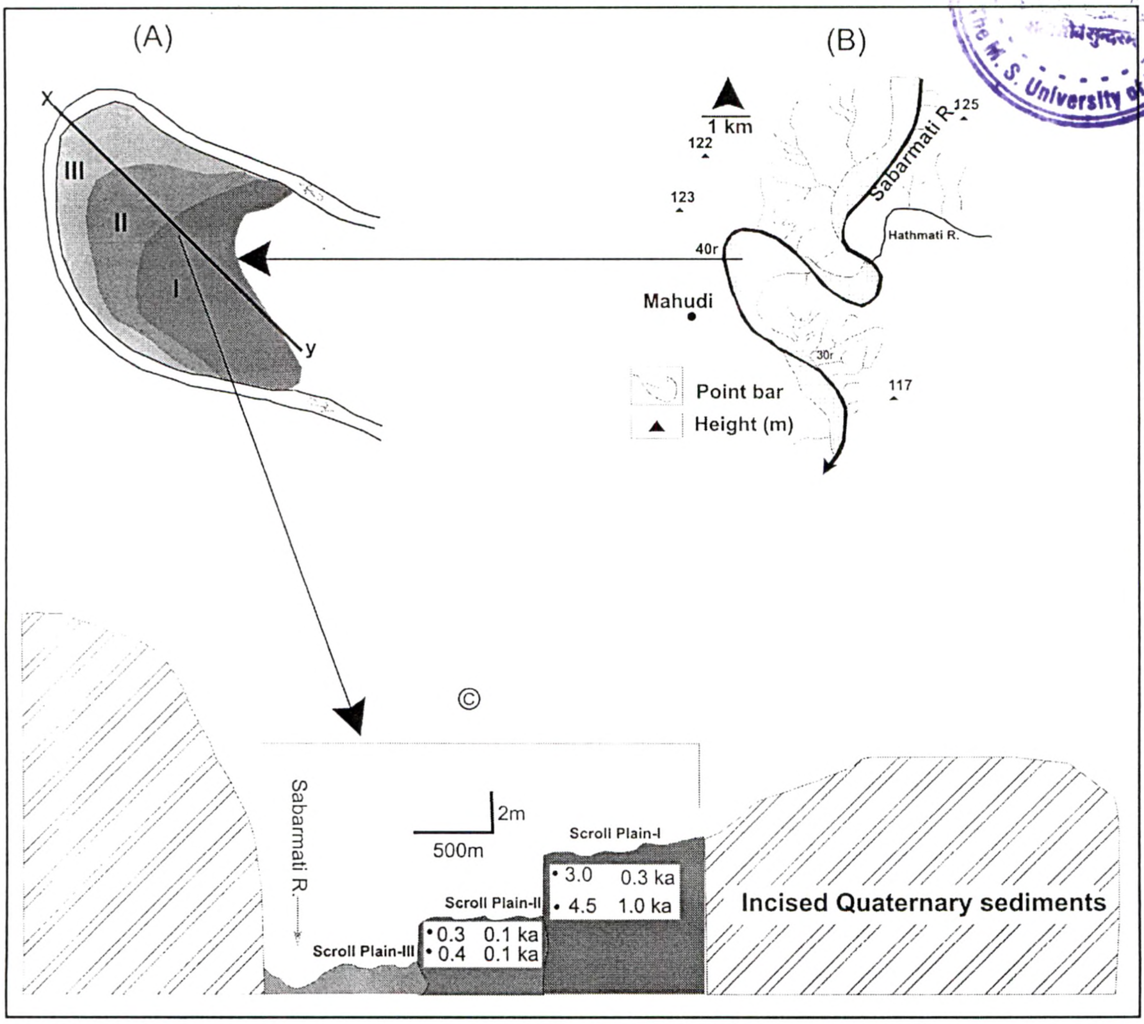

Figure-3.2. Scroll plain development at Mahudi in Sabarmati basin. (A) Scroll plain in the vicinity of Mahudi (B) section across the scroll plain and (C) vertical section of scroll plains with luminescence ages. (after Srivastava et al., 2001).

A 3.0 m thick sequence is exposed at the youngest edge of scroll plain-II in a quarry and is dominated by large-scale planar cross beds made up of coarse sand at the bottom, overlain by a trough cross-bedded unit. 5-10 cm thick dark coloured silty clayey bands towards the top separate this unit. Overall grain size is dominated by coarse to medium sand (average 1.16 ϕ), which is well sorted. A nearly 2 m thick sequence in scroll plain-III consists large-scale planar cross-beds. These beds are bounded by erosional surfaces. Grain size is dominated by medium sand (1 18ϕ), and the sediments are well sorted.

Depositional environment

The overall sediment characteristics of the upper fluvial sequence suggest its deposition in a low energy environment This is typical of flood plain fines facies element of Miall (1996) representing the sedimentation in a flood plain regime (Willis and Behrensmeyer, 1994). In addition to this, presence of bedded calcrete (Fig. 3.1, Mahudi-A), which are usually formed by ground water fluctuation in a riverine or playa environment (Goudie, 1983) also suggest that deposition took place in proximity of a channel McCarthy and Metcalf (1990) suggested that flood plains are most conducive for the formation of bedded calcretes where ground water remains generally closer to the surface in semi-arid areas and high evaporation leads to the development of such calcretes. The grain size assemblages show that the river has cohesive banks. Moderate pedogenesis in the upper part of the formation indicates landscape stability with reduced sediment supply and/or decreased flooding.

The aeolian sand overlies the upper fluvial sequence and is readily identified in the field due to its striking pale gray colour, friable nature and sharp basal contact. Very fine sand (88%) and silt+clay (12%) dominate the average grain size. The sediments are well sorted, finely skewed and occur as linear or crecentric ridges on the terrace surface.

Scroll plain formation takes place in laterally migrating meandering rivers with a consistent flow in relatively unconfined valleys having B3b type of flood plain channel (Nanson and Croke, 1992). In the Sabarmati River, the three well-defined scroll plains separated by distinct vertical offsets suggests formation of ingrown meanders, indicating adjustment to episodic uplift through incision (Holmes, 1972). Gradual enhancement of the palaeosinuosity shown by the measurements of the radius of curvature of scroll bars also indicates tectonic activity (Schumm, 1993). Coarsening of grain size from scroll plain-I to III also suggests an increased river gradient probably due to tectonism.

Chronology and palaeoenvironments

Table 3.1A, 3.1B and 3.2 provides the experimental data on samples from the upper fluvial and aeolian sequence and on scroll plain samples, respectively. Quartz ages obtained on sample MQ-1 to MQ-4 was based on the Australian slide method (Prescott et al., 1993) whereas for MQ-5 and MQ-6 the multiple aliquot additive dose (MAAD) method was used (Table-3.1A). Feldspar separates were also analyzed using the MAAD technique. The scroll plain samples (both quartz and feldspar extract) were also analyzed using additive dose protocol. Additionally the single aliquot additive dose (SAAD) technique was applied on quartz extract of 4 samples of scroll bars (Table-3.2).

Sample No	Depth (m)	U (ppm)	Th (ppm)	K %	Dose Rate (Gy/ka) Quartz	Dose Rate (Gy/ka) Feldspar
MQ-1	8.40	1.6±0.1	7.6±2.1	1.13±0.1	1.9±0.2	2.38±0.2
MQ-1A	8.50	3.0±1.0	11.5±3.3	1.44±0.1	2.6±0.3	3.15±0.3
MQ-3	3.40	1.1±0.3	5.8±1.1	1.05±0.1	1.6±0.2	2.09±0.2
MQ-4	2.60	2.1±0.4	4.0±1.2	0.96±0.1	1.6±0.2	2.10±0.2
MQ-5	1.20	2.2±0.7	9.6±2.6	1.11±0.1	2.1±0.3	2.78±0.3
MQ-6	0.70	2.1±0.3	2.9±1.2	1.55±0.1	2.2±0.2	2.66±0.2

Sample No.	Depth (m)	Ed (Gy) Quartz	ED (Gy) Feldspar	Age (ka) Quartz	Age (ka) Feldspar	Mean age (ka)
MQ-1	8.40	124±16	98±3	66±12	41±4	54±6
MQ-1A	8.50	106±14	117±9	40±7	37±5	39±5
MQ-3	3.40	50±10	86±9	32±7	41±5	37±5
MQ-4	2.60	74±20	69±1	46±13	33±3	40±13
MQ-5	1.20	61±12	87±7	29±7	31±4	30±8
MQ-6	0.70	31±3	23±2	12±2	9±1	12±2

Cosmic ray dose 150μ Gy/a. Water content considered 15±5%

Table 3.1A Experimental details and luminescence ages obtained on upper fluvial sequence in the Sabramati River basin using MAAD technique.

Sample No	Depth (m)	U (ppm)	Th (ppm)	K %	Dose Rate Gy/ka (Quartz)	Dose Rate Gy/ka (Feldspar)
1A	2.40	1.0±0.5	8.5±2.0	1.2±0.1	1 8±0 2	2.3±0.2
1B	1.20	1.0±0.4	5.2±1.2	2.1±0.1	2.4±0.2	2.9±0.21
2A	2.15	1 0±0.7	10.5±3.0	2.2±0.2	2.8±0.3	3.3±0.3
2B	1.65	1.3±1.1	14.4±4.0	2.4±0.1	3.3±0.4	3.8±0.4

Sample No	Depth (m)	ED (Gy) Quartz	ED (Gy) SAAD	ED (Gy) Feldspar	Age (ka) Quartz	Age (ka) Feldspar	Age (ka) SAAD
1A	2 40	6.7±2.4	8.2±0.8	9.8±1.7	4±1	4±1	4.5±1
1B	1.20	8.8±0.1	6.5±0.5	16.6±1.2	4±0.3	6±0.6	3.0±0.3
2A	2.15		1.06±0.2	11.4±1.5		3±0.5	0.4±0.1
2B	1.65		0.9±0.2	2.5±0.4		0.7±0.1	0.3±0.1

Cosmic ray dose 150μ Gy/a. Water content considered 15±5%

Table 3.1B Experimental details and luminescence ages obtained on scroll plain sequence in the Sabramati River basin using MAAD technique.

Aliquot	Palaeodose (Gy)			
	1A	1B	2A	2B
1	8.0±1.0	7.1±0.8	2.9±0.6 [a]	1.3±0.1
2	10.6±1.1 [a]	11.5±2.7 [a]	5.9±0.8 [a]	4.3±0.3 [a]
3	8.4±1.2	2.9±0.5 [a]	0.9±0.2	1.5±0.1
4	23.3±4.9 [a]	6.8±1.0	1.0±0.2	1.2±0.1
5	16.6±3.2 [a]	5.9±1.2	1.5±0.5	0.7±0.0
6	16.1±3.6 [a]	6.4±0.8	1.4±0.4	0.8±0.1
7	12.9±1.2 [a]	5.9±0.8		0.7±0.1
8	8.63.5			1.1±0.1
Weighted Mean	8.2±0.8	6.5±0.5	1.1±0.2	0.9±0.2

Cosmic ray dose 150μ Gy/a Water content considered 15±5%

Table 3.2 SAAD palaeodose obtained on scroll plain in the Sabarmati River basin.

Within the measurement errors, the overall concordance of the BGSL and IRSL ages on samples from the upper fluvial sequence and aeolian sand suggests that in general, these samples are sufficiently bleached. With this premise, the luminescence ages of sample MQ-1 (basal sample) and MQ-5 (topmost sample) should represent the onset and termination of the last fluvial phase in the Sabarmati basin. Sample MQ-6 from aeolian sand overlies MQ-5 and represents the timing of the onset of aeolian activity at this site. In view of the overall concordance of the BGSL and IRSL ages, their weighted means have been used for discussion. At Mahudi, the beginning of the fluvial sedimentation above red soil (red bed) is dated to 54±6 ka (Fig. 3.1, Mahudi-A, sample MQ-1). A stratigraphically equivalent sample (MQ-1A) from a rain gully, 5 km inland, gave an age of 39 ±5 ka (Fig. 3.1, Mahudi-B) This sample is from a channel sand body overlying the red soil. In view of the fact that sedimentation in a channel can be truncated, as compared to the continuously aggraded flood plain (such as at Mahudi), the younger age of the rain gully sample may reflect erosion of the earlier record. Luminescence ages on MQ-1 and MQ-5 suggest that at Mahudi, aggradation of the upper fluvial sequence commenced at ~54 ka and terminated at 30 ka (Fig. 3.1, Mahudi-A).

Aeolian sedimentation commenced at 12±2 ka after a hiatus of ~20 ka. at Mahudi. A slight discrepancy between the IRSL and BGSL ages for the dune (Table-3.1A, sample MQ-6) does not alter the overall conclusion that there was a prolonged hiatus between the cessation of the fluvial aggradation and onset of aeolian accumulation. Evidence of pedogenesis in the upper part of the fluvial sediments also supports this inference. The hiatus occurred between 30±8 ka and 12±2 ka, and reflects the fact that the geomorphic activity (with respect to net aeolian and fluvial aggradation) during this period was subdued (Fig. 3 1, Mahudi-A) Kar et al. (2000) derived similar inferences based on a detailed study of a sequence in the Thar Desert.

Out of three scroll plains, only two (I and II) yielded sufficient amounts of the desired size fraction for dating The feldspar ages of scroll plains are somewhat overestimated compared to SAAD ages on Quartz, suggesting a marginally poor bleaching of the feldspar fraction (Table-3.1B). In absolute age terms, the difference is not significant but the differences indicate that these ages are on the limits of the dating method In view of this, the SAAD ages have been used in the discussion on the evolution of the scroll plains Table 3.2 summarizes the data on the scroll plains. Scroll plain-I yielded SAAD ages of 4.5±1 ka (1A) and 3±0.3 ka (1B). Scroll plain-II yielded SAAD ages of 0.4±0.1 ka (sample 2A, 2.15m) and 0.3±0.1 ka (sample 2B, 1.65m). Being from the upper part, these ages represent the terminal phases of the scroll bar aggradation.

Sequences identical to the upper fluvial sequence are reported from many localities in north Gujarat (Wasson et al., 1983; Sridhar et al., 1994; Tandon et al., 1997; Chamyal et al., 2003). It has been suggested that an extensive fluvial system was operating in the region during the deposition of the upper fluvial sequence. The deposition of about 7.5 m of silty sand during this period implies a persistent hydrological regime. The fluvial aggradation commenced around 54 ka and continued till 30 ka. Absence of any weathered horizon in the sequence suggests that fluvial aggradation was continuous and the presence of bedded calcretes suggests fluctuating ground water, indicating seasonality (McCarthy and Metcalfe, 1990). Termination of fluvial aggradation was followed by a prolonged phase of non-deposition and moderate pedogenesis in the upper part. The fluvial sequence is overlain by extensive dune sand, which is around 1-3 m thick Along the Sabarmati

River at Mahudi, it has been dated to 12 ka. However, earlier ages of aeolian sand from this region range from 20 ka to 5 ka (Wasson et al., 1983; Tandon et al., 1997). This suggests that the aeolian sedimentation at Mahudi either commenced after a hiatus of 10-20 ka or older dunes are not preserved. However, the termination of dune building activity occurred around 5 ka.

Mahi Basin

Except for the Rayka section (Juyal, 2000) where aeolian sand directly overlies the red soil, the regional stratigraphy based on a number of exposed sections down stream of Rayka show that aeolian sedimentation did not appear in the basin immediately after the formation of red soil. Instead, a renewed phase of fluvial aggradation followed after the development of red soil as suggested by the presence of fluvial sediments above red soil (Merh and Chamyal. 1997). Towards the upper part it becomes fluvio-aeolian sand and is finally succeeded by dominantly aeolian sand towards the top. These sediments above the red soil have not been studied in detail for sedimentological and chronometric studies. Since the present work was aimed at understanding the upper fluvial sequence (last fluvial phase) in the region, an attempt has been made to document in detail the sedimentary sequence overlying the red soil in the alluvial plain of the Mahi basin. Stratigraphically constrained samples are luminescence dated in order

to ascertain the timing of last major fluvial activity. The onset of arid phase in the basin is estimated by dating the upper aeolian sand. In the present study five sections have been investigated and their stratigraphic details are given in figure 3.3.

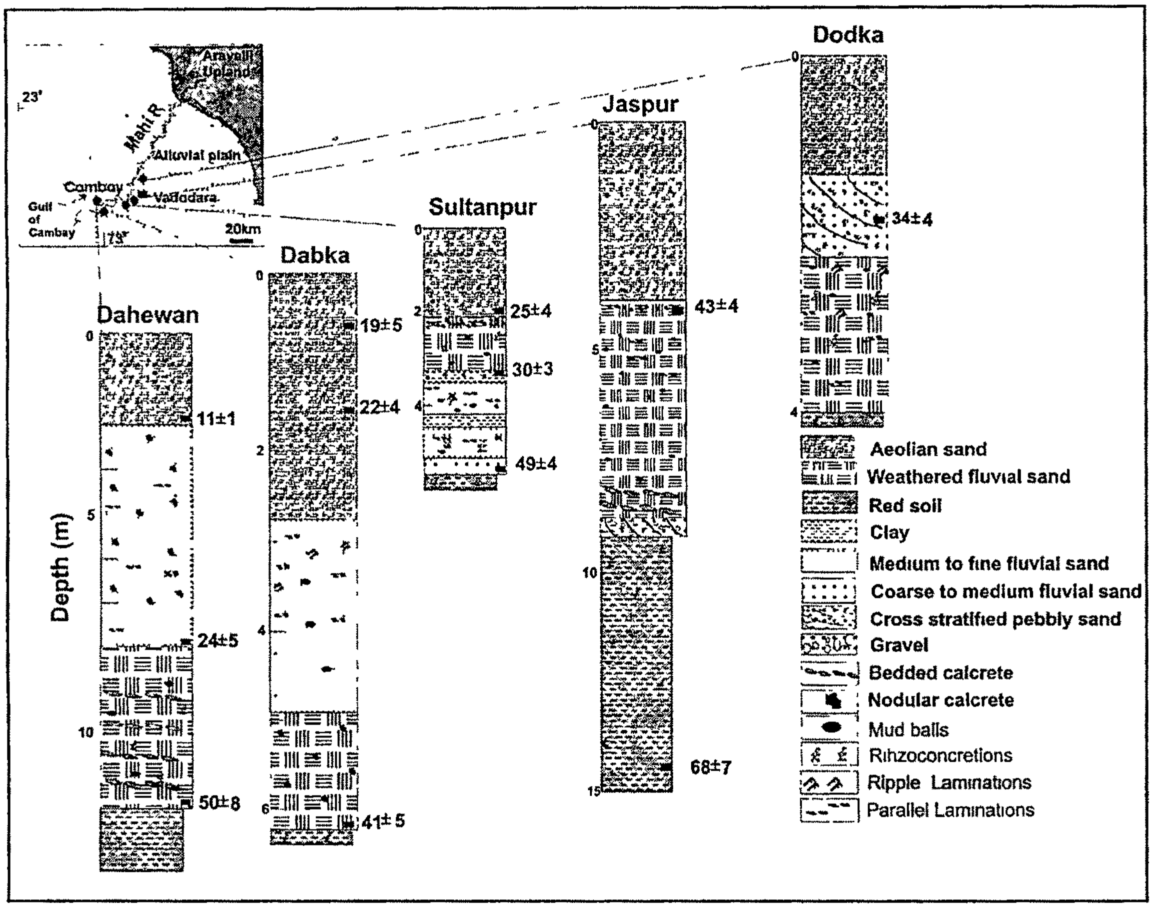

Figure-3.3. Stratigraphy and luminescence chronology of fluvial and aeolian succession above red soil.

(a) ***Dodka:*** A 4 m thick sequence is exposed in a rain gully near Dodka village (Fig. 3.3; Dodka). A 1.5 m thick weathered horizon lies immediately above the red soil. Sediments are dominated by fine sand containing occasional basalt pebbles. Presence of nodular and tubular calcretes is seen dispersed in the horizon. However, at places it has preserved faint parallel and ripple laminations. This is overlain by 1 m thick trough cross-stratified gravel dominated by basalt, calcretes and occasional quartzite clasts. The amplitude of the troughs decreases towards the top with a preferential dip due south. This is overlain by 1.2 m thick buff coloured aeolian sand with friable carbonate concretions towards the top.

(b) ***Jaspur:*** A 15 m thick section is exposed on the left bank of Mahi near Jaspur village (Fig. 3.3; Jaspur). At this location, the thickest red soil horizon (~6m) in the Mahi basin is found resting on a calcrete bed. The red soil is dominated by fine sand with discrete occurrence of pebbles in the horizon. The horizon shows evidences of postdepositional weathering and pedogenesis as indicated by the blocky character of the sediments with well developed ped faces and widely distributed nodular and tubular calcretes. At places pebble lenses are also encountered. This is overlain by a thin (50 cm) channel gravel. This is followed by a 5 m thick weathered grey very fine sand similar to Dodka. The lower part has preserved fossil mud balls, bedded calcrete, and faint parallel laminations. In the upper part, sediments are pedogenised with a distinct occurrence of concretionary carbonate. A 4 m thick aeolian sand that show a gradational contact overlies this.

(C) ***Sultanpur:*** A 5 m thick sequence overlying the red soil is exposed on the left bank of Mahi River (Fig. 3.3; Sultanpur). Immediately above the calcretised red soil, a 30 cm thick gritty sand with cross lamination was deposited. This is overlain by 2 m thick sequence comprising two units showing parallel and ripple laminated fine to very fine sand (2.58-3.36ϕ, 97%) that are invariably capped by fractured clay. At places secondary carbonate in the form of nodules and rhizoliths are seen dispersed in the sand layers. This horizon is overlain by 1 2 m thick weathered, fluvially reworked fine aeolian sand (2.95ϕ, 99%). The horizon is massive, with nodular and tubular calcrete. Towards the top, nodular calcrete forms a distinct 30 cm thick horizon, suggesting local reworking by fluvial process. At some places the horizon is interspersed with basaltic pebbles. The sequence ends with the deposition of 2 m thick friable fine aeolian sand (2.68ϕ, 99.5%) which is pale yellow in colour.

(d) ***Dabka:*** A 6 m thick sequence above silty clay rich red soil is exposed along the left bank of Mahi River at Dabka village (Fig. 3.3; Dabka). Immediately above the red soil is 1 m thick silty sand that shows evidence of moderate pedogenesis. This is overlain by 2 m thick weakly pedogenised silty sand. At places distinct fluvial features like parallel and ripple laminations and mud balls are well preserved. The sequence ends with 2 5 m thick buff coloured friable aeolian sand towards the top.

(e) ***Dahewan***: A 12 m thick sequence is exposed at the right bank of Mahi River near Dahewan village (Fig. 3.3; Dahewan). At this locality distinction of red soil is not very clear due to salt encrustation caused by periodic ingression of saline water in the Mahi estuary from the Gulf of Cambay during high tides. However, based on the regional correlation with other sections, the bottom horizon with well-developed pedality suggests it to be the red soil. This is followed by a 3.5 m thick moderately weathered horizon containing well developed bedded calcrete bands. The sediments are dominated by very fine sand (3.66ϕ) that constitute 68%, followed by silt (12%) and clay constitute the remaining 20%. Calcrete bands show a rhythmic appearance and protrude out in the vertical section due to differential erosion. This horizon is overlain by 2 m thick moderately weathered very fine sand (3.56ϕ, 84%) with occasional pebbles. Contrary to the lower horizon, it shows evidence of weak weathering towards the upper part with the dominance of nodular calcretes. Besides this, faint parallel laminations are preserved in this horizon suggesting evidence of weak fluvial activity before the deposition of upper 2 m thick very fine aeolian sand (3.25ϕ, 95%). Contact between the aeolian sand and underlying horizon is gradational

Depositional environment

Sediments constituting the red soil are dominated by fine sand and occasional basaltic pebbles can be attributed to its deposition during the waning stage of sheet floods (Stear, 1983). In general, the sheet floods are incompetent to carry coarse bed-load. However, presence of pebble lenses suggest localized channel activity. Event of reddening is subsequent to the deposition and is usually found associated in the sediments of flood plain Broadly the red colour indicate better-drained sites in the flood plain reflecting higher elevation and/or permeable parent material (Kraus, 1997). In Mahi basin, red soil developed during periods of oxidation and soil drying, probably associated with a falling water table or good drainage (Juyal et al., 2000). Dry Land Rivers are largely ephemeral in character, and from a process point of view, they are primarily selective transporter, burial and re-excavation of their own sediments under episodic flows. Such rivers are subjected to frequent flood events of irregular and short duration that lead to the deposition of assorted wash and bed load material (Thornes, 1994, Knighton and Nanson, 1997, Graff, 1988). Following the development of red soil, climate temporarily reverted back to drier condition as indicated by the overlying trough cross-stratified sandy gravel. However, this event was short lived and localized. Discrete occurrence of planar and cross-stratified gravel dominated by poorly sorted clasts of basalt, quartzite and calcrete at Dodka, Jaspur and Sultanpur suggest sudden increase in sediment supply. This could happen in arid and semi-arid environment where episodic storm surge events are common during which rivers are capable of eroding and transporting sediments from poorly vegetated catchment (Graf, 1988). This gives rise to braided channel system having typically large width to depth ratio in which the number of individual channels can vary from 1 to more than 20 (Thornes, 1994). In a rare event the river bed is completely occupied, however in a given time the distributary channels carry water and are known for frequent migration of channels that lead to bank erosion. Presence of rolled carbonate nodules indicate the ability of the flow to erode pre-existing alluvial carbonate from the banks, probably caused by migrating channels. However, in view of its limited extent, it can be suggested that the event was short lived and local in nature

A persistent fluvial regime reappears in the basin with the deposition of fine silty sand usually overlying the red soil (Fig 3.3). Distinct fluvial signatures are preserved in the form of current/ripple laminations and mud balls suggesting prevalence of low energy meandering river system. The deposits are typical of flood plain fines facies of Miall (1996) representing the sedimentation in a flood plain regime (Willis and Behrensmeyer, 1994). These sediments are at times associated with the bedded calcrete for example at Jaspur, and Dahewan. Bedded calcrete formation is usually related to the ground water fluctuations in a riverine playa environment (Goudie, 1983), thus suggesting its deposition proximal to a channel. It has been further suggested that flood plains are most conducive locations for the development of bedded calcretes where ground water remains close to the surface in semi-arid areas, thus a high evaporation is ensured leading to its development (McCarthy and Metcalf, 1990). Therefore, a vertical aggradation of this facies that varies in thickness ranging from 2-10 m suggests that the deposition was facilitated under a persistent flow regime under well-defined channel (e.g. meandering course) with periodic over spilling of silty sand on to the adjacent floodplains. Evidence of moderate pedogenesis associated with these sediments suggests phases of non-deposition when the channel responsible for the flood plain aggradation migrated laterally. Such channel migration occurs under changing water budget (both increasing and decreasing). In either situation, river tends to abandon the old course and occupies the new one. This led to the exposure of the flood plain sediments for sub-aerial weathering a process responsible for the development of flood plain soils (Kraus and Aslan, 1993). In the foregoing it is evident that the sediments above the red soil have been deposited under improved moisture availability, which led to the formation of cohesive banks due to the growth of vegetation and restricted the sediment supply only during the peak flood events. The overlying aeolian sand shows gradational contact with the underlying fluvial horizon. This indicates initiation of drier climatic condition, which could be associated with enhanced wind activity in the region

Chronology and palaeoenvironments

A preliminary data on chronology is obtained for the Rayka section by Juyal et al., (2000). Based on IRSL and BGSL ages it has been suggested that fluvial aggradation in the Mahi basin began after the retreat of last Interglacial high sea level. Thus, for the first time the bottom marine clay was assigned an age of 125 ka (Last Interglacial). Two episodes of fluvial aggradation, one between Gravel-I and II and second above Gravel-II, are assigned Marine Isotopic Sub-Stage-5 (extrapolated age-estimate) and the second event is dated to 50-30 ka and corresponds to Marine Isotopic Stage-3 (MIS-3). It has been suggested that MIS-3 reflect a more humid environment and is seen in both regional and global context. Luminescence chronology bracketed the red soil age between 40-25 ka. In the present study, all the samples were analyzed using the single aliquot BGSL protocol of Murray and Wintle, (2000). Table-3.3 provides the experimental data on samples from the Mahi basin that are dated from the sequence above the red soil. However, at Jaspur one sample is dated from the red soil itself (sample MJ). This sample yielded an age of 68±7 ka. An earlier age estimate based on weighted mean age by Tandon et al (1997) assigned 58±5 ka for red soil in Sabarmati basin. Within the errors, the ages are broadly in agreement with the age obtained by Tandon et al. (1997) Sediments corresponding to the upper fluvial sequence (above the red soil and below the aeolian sand) are bracketed between 50±8 and 30±3 ka. There is no appreciable hiatus seen between the termination of upper fluvial regime and commencement of aeolian sedimentation in the basin. Based on the field stratigraphy and the luminescence chronology it can be said that aeolian sedimentation started around 30 ka in the region.

Comparison of quartz BGSL and feldspar IRSL ages suggest underestimation of IRSL ranging from 7% to more than 50% (Fig. 3.4, Table-3.4). However, on red soil the underestimation is around 13 % (Table-3.4, sample MJ). Comparing the earlier IRSL age on red soil (40 ±10 ka =50 ka) at Rayka (Juyal, et al., 2000) with that of the stratigraphically equivalent BGSL age on red soil at Jaspur (68±7 ka= 61 ka) suggest an underestimation of around 18% in IRSL age obtained at Rayka.

Jaspur

Sample No.	Depth (cm)	U (ppm)	Th (ppm)	K (%)	H_2O	Dose rate (Gy/ka)	ED (Gy)	Age (ka)
MJ-2	800	2.0±0.4	7.3±1.4	1.3±0.1	10±5	2.2±0.2	95±1	43±4
MJ	1900	1.4±0 2	4.0±0.5	1.4±0.1	10±5	1.9±0.1	135±8	68±7

Sultanpur								
MS-5	200	2.9±1.2	8.6±4.1	1.4±0.1	10±5	2.6±0.4	60±1	23±4
MS-4	320	3.6±0.8	15.2±3.0	1.2±0 1	10±5	3.0±0.2	89±1	30±3
MS-1	520	1.4±0.4	6.6±1.3	1.2±0.1	10±5	2.0±0.2	95±1	49±4
Dodka								
TR-236	380	2 3±1.0	13.0±3.0	1.1±0.1	10±5	2.5±0.3	85±1	34±4
Dabka								
TR-238	800	2.3±1.0	8.4±2.0	1.6±0.1	10±5	2.6±0.3	107±1	41±5
Dahewan								
MD-5	200	3.4±0.5	12.4±2.0	1 3±0.1	10±5	2.8±0.2	32±1	11±1
MD-4	700	2.3±1.4	17.5±5.0	1.0±0 1	20±5	2.4±.0.5	56±1	24±5
MD-2	1100	2.2±0.5	7.7±1.8	1.3±0.1	20±5	2.0±0.2	82±1	50±8

Cosmic ray dose 150μ Gy/a

Table 3.3 Experimental detail and single aliquot BGSL ages obtained on fluvio-aeolian sequences in the Mahi River basin.

Sample No.	BGSL (Age ka)	IRSL (Age ka)	% Underestimation in IRSL	Sediment Type
MSD-4	17±1	10±1	41	Aeolian
MSD-1	22±2	17±2	22	Aeolian
OA-4	21±2	14±1	33	Aeolian
MJ-2	43±4	40±3	7	Fluvio-Aeolian
MJ	68±7	59±5	13	Fluvial (Red Soil)
MS-4	30±3	23±2	23	Fluvio-Aeolian
OB-4	21±2	14±1	33	Fluvio-Aeolian
MS-1	49±4	30±2	39	Fluvial
OA-3	60±6	31±3	48	Fluvial
OA-2	69±6	39±3	43	Fluvial
OA-1	97±8	47±4	51	Fluvial

Table 3.4 Comparison of single aliquot BGSL and multiple aliquot IRSL ages.

Luminescence dating provides the age estimate for the time of sediment deposition, hence it can be inferred that red soil formation occurred after around 60 ka in the Mahi basin (Fig. 3.3). The BGSL chronology indicates that the resumption of low energy fluvial regime followed after a hiatus possibly caused by the weakening of fluvial regime. As a consequence, during the period of non-deposition, red soil development occurred in the basin. A conservative estimate based on the age difference between the red soil and the overlying fluvial sediments suggests that the subdued fluvial regime prevailed for a period of ~10 ka (subtracting the upper fluvial sequence age of 50 ka from red soil

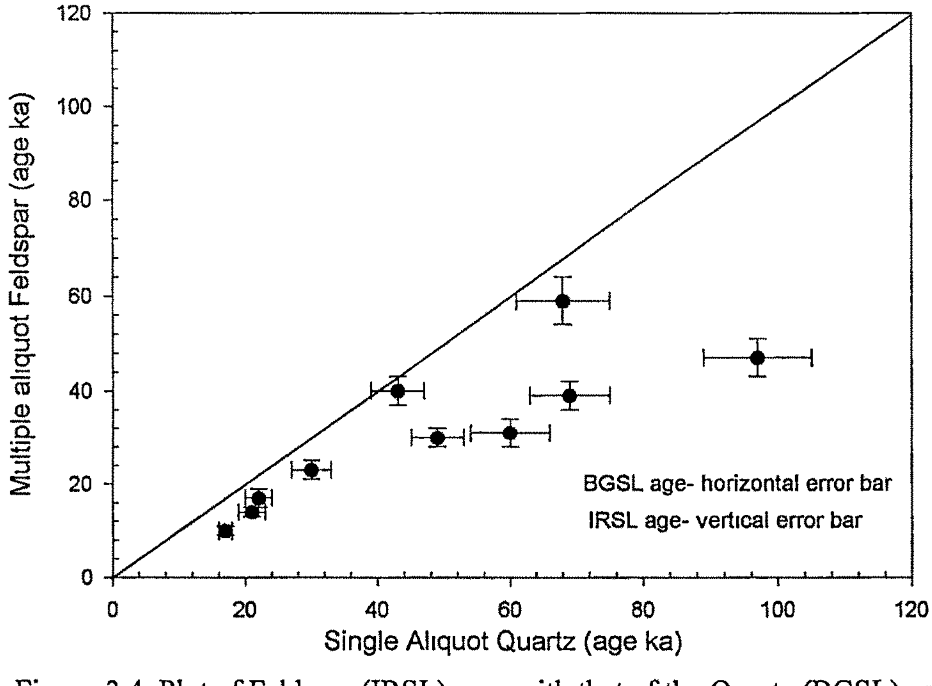

Figure-3.4. Plot of Feldspar (IRSL) ages with that of the Quartz (BGSL) ages obtained on the same samples in Mahi and Orsang basins.

age of 60 ka). It was only after around 50 ka that a persistent fluvial regime re-established in the region. That led to the aggradation of silty sand showing varying degree of weathering/pedogenesis. Presence of bedded calcretes in this horizon indicates that fluvial activity was not monotonous but punctuated by fluctuating hydraulic discharge. Towards the upper part, dominance of very fine sand indicate that there was a subordinate aeolian component getting admixed with the weak fluvial regime. At times episodic surges of storm events were capable of depositing a large flux of assorted sediments as seen at Dodka and Sultanpur (Fig. 3.3). Though such events were localized, BGSL age ranging between 34-30 ka suggest that the climate was getting steadily drier in the region. Finally the full aeolian environment began around 25 ka. however, at Jaspur an older age of 32 ka has been obtained.

Orsang Basin

Orsang is the only river that constitutes the part of Lower Narmada basin in the study area and does not drain into the Gulf of Cambay; instead it meets the Narmada River at Chandod (Fig. 1.1 and 1.2). In its lower alluvial tract (~20 km) the Quaternary sediments are exposed along both banks. Two such sections between Bahadarpur and Chandod are investigated for reconstructing the Quaternary stratigraphy (Fig. 3.5).

(a) ***Bahadurpur:*** A 20 m thick sequence is exposed along the right bank of Orsang River near Sankheda bridge at Bahadurpur (Fig. 3.5). The sequence begins with 1.5 m thick fractured mottled clay showing evidence of calcretization at the bottom. This is followed by 1.5 m thick trough cross-stratified gravel dipping towards SW and is dominated by quartzite, granite and calcrete clasts (~20 cm). This gravel has an erosional contact with the underlying silty clay. This is succeeded by 4 m thick gritty sand showing crude lamination. Overlying this horizon is a 4 m thick horizon that shows evidences of pedogenesis, however at places faint parallel laminations, mud balls and 5-10 cm thick channel sand bodies may be seen The horizon shows blocky structure and clay illuviation along the ped faces. The grain size is dominated by very fine sand (3.2ϕ, 68%) followed by clay 21% A 6.5 m thick multistoried channel sand body that has scoured the underlying horizon overlies this. In the field, four individual units can be discerned ranging in thickness between 1 to 2 m showing fining upward sequence that are invariably capped by mud drapes. Besides this, all units show faint parallel and ripple laminations and contain mud balls and friable rhizoconcretions. The sand dominated horizon show dominance of fine sand (2.4ϕ) that varies between 80-97%. This is overlain by a 2 m thick fluvio-aeolian sequence that is finally succeeded by 2 m thick aeolian sand towards the top.

(b) ***Aritha:*** A 20 m thick section is exposed on the left flank of Orsang River at Aritha village (Fig. 3.5). From bottom upward a 2 m thick greyish yellow fractured sandy silty mud containing tubular rhizoconcretions is seen. Following this is a 1.5 m thick SSW dipping trough cross-stratified gravel horizon dominated by the clasts (~15 cm) of quartzite, calcrete and granite. A suspected Lower Middle Palaeolithic tool was found ~1 km upstream of Aritha from this horizon that was embedded in the pebbles. This horizon occurs as lensoidal body. This is overlain by 4.5 m thick reddish yellow sand with distinct bands of bedded calcretes occurring at regular spacing of 10-20 cm Grain size show presence of vary fine sand (3.1ϕ, 67%), silt (19%) and clay (12%). The horizon is moderately weathered and fairly compact. This is overlain by 4 m thick equally proportionate very fine sand (48%) and silt

(45%). At places occasional sandy channel gravels may be seen. The horizon shows moderate weathering along with the presence of nodular calcrete and overlain by channel sand towards the top. This is succeeded by 3.5 m thick horizons of pedogenised silty sand showing blocky structure along with nodular calcretes (5-10 cm) occurring towards the upper part of this horizon. Illuviated clay is found as coating along the ped faces. This is overlain by 4.5 m thick very fine aeolian sand that has evidences of moderate pedogenesis towards the upper part.

Depositional Environment

Stratigraphy of the exposed sediments indicates a phase of regionally extensive fine silty clay deposition in the basin and is seen between Bahadurpur and Chandod (Fig. 3.5). The sedimentary structures have been obliterated due to the subsequent weathering and pedofaunal activity, however, the texture of the sediments suggests that the deposition occurred in a low energy fluvial regime, possibly in a distal flood plain environment. The overlying trough cross-stratified, assorted gravel indicates deposition of sediments as bedload, a characteristic feature of Dry Land Rivers. Mobilization of sediment in such rivers is associated with the rising limb of flood hydrograph (scouring) and the deposition facilitated during the flood recession phase (filling). Such scouring and refilling give rise to trough cross-stratification and operate both in sand-bed and gravel-bed rivers of dry land (Hassan, 1990, Tooth, 2000). Termed as Gt facies by Miall (1996), their presence in Orsang River basin suggests the existence of braided river system with large width/depth ratio and easily erodable banks (Thornes, 1994). Furthermore, the lateral swelling and pinching of this horizon indicates presence of distributary channel system suggesting frequent migration of the channel in order to adjust with the fluctuating water budget. Such deposition is facilitated under highly irregular flow regime (ephemeral flow). Overlying fine silty sand with bedded calcrete at Aritha (Fig. 3.5) suggests that the fluvial system gradually transformed from braided to a low sinuosity channel (Schumm and Brakenridge, 1987). This may have caused by less catastrophic rainfall induced run off events due to the protection of the catchment and river banks by the growth of vegetation (Miall, 1996). McCarthy and Metcalf (1990) suggested that flood plains are most conducive for the formation of bedded calcretes where ground water remains generally closer to the surface and high evaporation leads to the development of such calcretes (in semi-arid areas). Thus, overall this horizon indicates well-developed floodplains with occasional overtopping of the banks- caused in low to medium sinuosity meandering flow regime. This horizon is missing at Bahadurpur, instead a gritty sand directly overlies the trough cross-stratified horizon (Fig. 3.5, Bahadurpur). The assorted nature of sediment in this horizon suggests presence of a wide, shallow, steep braided bed load channel. The deposition occurred during the events of episodic high-energy floods that is typical of ephemeral rivers. Similar horizon, though texturally bit finer and better sorted along with sandy gravel channel deposits overlies the bedded calcrete at Aritha (Fig. 3.5). Process point of view it appears that this was deposited under similar climatic condition as that of the gritty sand horizon at Bahadurpur.

The succeeding horizon is pedogenised silty sand with mud balls and nodular calcrete. This horizon suggests that the fluvial discharge had not only reduced in terms of its carrying capacity but also became well regulated with less frequent stormy events. In view of the fact that grain size is well sorted and finer, it indicates that deposition took place away from the channel in a low sinuosity meandering stream possibly on flood plain environment. Overall deposition occurred under more persistent flow regime.

Overlying this horizon at Bahadurpur are four distinct units of fining upward sequences rest over the scoured base indicating a flashy character of the fluvial system (Fig 3.5, Bahadurpur) Its absence at Aritha could be due to the localized nature of the event that could have been deposited by the tributary streams, possibly the anabranch of the main trunk river. The ambient channel responsible for the deposition of this horizon gradually eroded the underlying horizon in order to reach the base level of the trunk river. Deposition of the scoured base occurred during high flood events. The fining upward sequence in these units suggests receding sedimentation in a meander cut-off or a flood outlet of a major ephemeral stream during episodic high flood events (Kar et al., 2001). The succession is overlain by fluvio-aeolian sediments suggesting placid sedimentation with the decrease in water budget caused by the initiation of drier climate. A drier climate sets in with the initiation of aeolian sedimentation towards the top.

Chronology and palaeoenvironments

Table-3.5 gives the experimental data on the samples analyzed from Orsang basin. Luminescence chronology of the Bahadurpur section (Fig. 3.5) show that the gritty sand above the trough cross-stratified gravel is 63±5 ka old whereas the overlying pedogenised very fine sand gave an age of 49±4 ka. Following this four fining upward channel sand units provided dates of 25±3 (at 1050 cm depth) and 23±2 ka (at 500 cm depth) respectively. The overlying aeolian sand is dated to 21±2 ka. At Aritha (Fig. 3.5) the bedded calcrete horizon that overlies the trough cross-stratified gravel has been dated to

97±8 ka. The overlying medium to fine sand horizon with channel sand bodies is dated between 69±6 to 61±6 ka and the uppermost aeolian sand is dated to 21±2 ka (Fig. 3.5).

Based on the facies architect and available chronological data, it can be inferred that regional pluvial phase represented by bottom silty clay prevailed in the basin. The sediment texture suggests its deposition under persistent flow, though no direct age estimate is available on this horizon. The overlying bedded calcrete horizon at Aritha dated to 97±8 ka suggests that the underlying silty clay would have deposited during the Marine Isotopic Stage-5e (MIS- 5e). Following this the trough cross-stratified gravel that is sandwiched between the silty clay and bedded calcrete can be bracketed between <125 to >97 ka (Fig. 3.5, Aritha). This period correspond to drier climatic condition of MIS-5d (Bradley, 1985, Martinson et al., 1987) during which Orsang River was a low sinuosity channel carrying significant amount of bed load.

Bahadurpur

S.No.	Depth (cm)	U (ppm)	Th (ppm)	K (%)	H_2O (%)	Dose Rate (Gy/ka)	Ed (Gy)	Age (Ka)
OB-5	200	2.0±0.5	7.2±2.0	1.2±0.1	10±5	2.1±0.2	53±1	21±2
OB-4	600	3.1±1.2	27.0±4.0	3.1±0.2	10±5	5.3±0.5	115±2	23±2
OB-2	1050	1.1±0.5	29.0±4.0	2.4±0.1	10±5	4.4±0.4	102±1	25±3
OB-1B	1150	2.2±0.4	6.2±1.3	1.2±0.1	10±5	2.0±0.2	100±1	48±4
OB-1A	1450	1.7±0.4	7.5±1.3	1.4±0.1	10±5	2.2±0.2	139±1	62±5

Aritha

OA-4	600	2.0±0.4	6.7±1.4	1.3±0.1	10±5	2.1±0.2	46±1	21±2
OA-3	850	3.0±0.7	11.2±2.3	1.7±0.1	10±5	3.0±0.3	183±3	61±6
OA-2	1250	1.7±0.4	5.8±1.2	2.2±0.1	10±5	2.8±0.2	196±2	69±6
OA-1	1700	2.7±0.3	6.4±1.8	1.9±0.1	10±5	2.8±0.2	278±3	97±8

Cosmic ray dose 150μ Gy/a

Table 3.5 Experimental detail and single aliquot BGSL ages obtained on fluvio-aeolian sequences in the Orsang River basin.

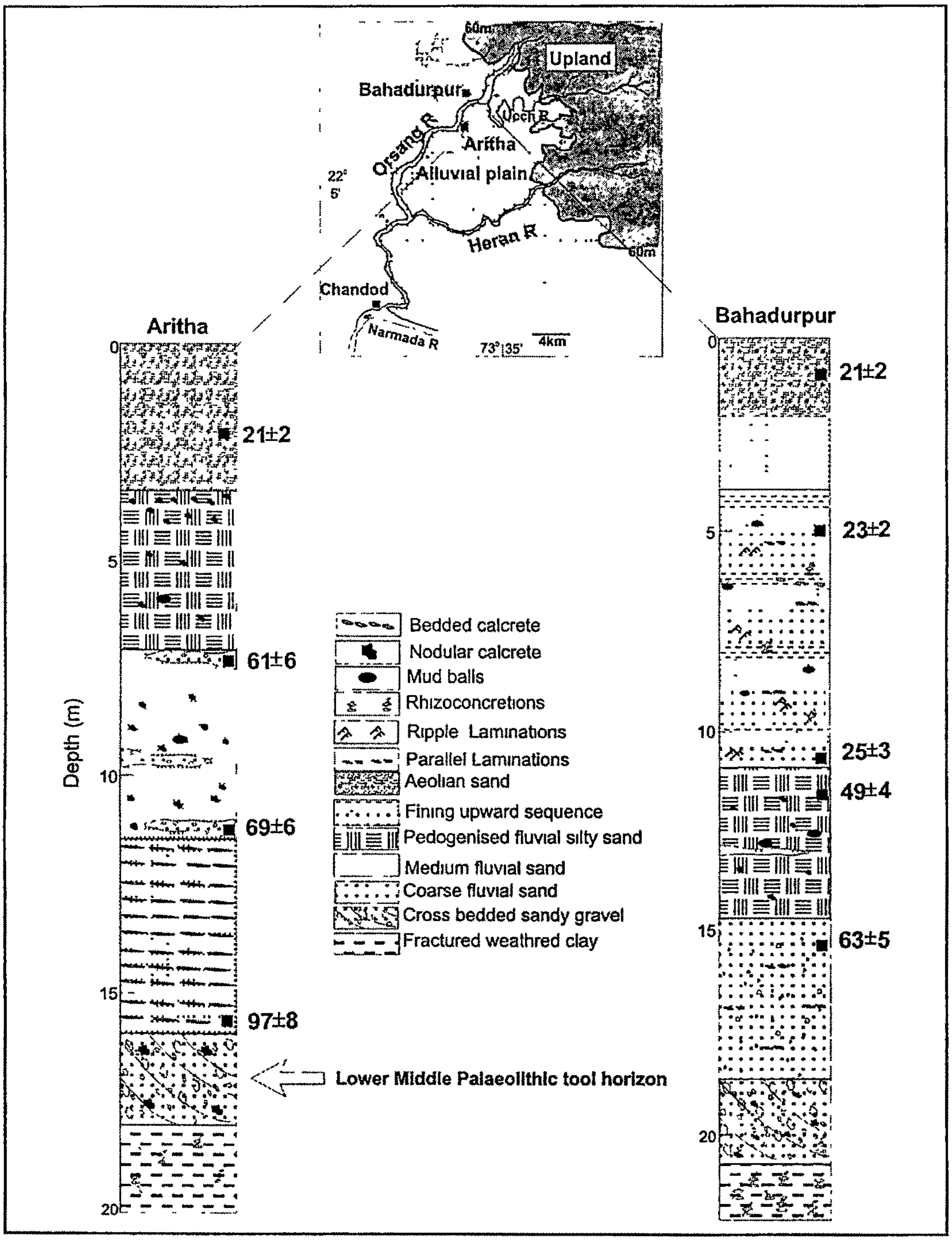

Figure-3.5. Stratigraphy and luminescence chronology of fluvial and aeolian sequences at Bahadurpur and Aritha in Orsang basin.

Interestingly, the suspected Lower Middle Paleolithic tool that was obtained from the trough cross-stratified gravel can be placed anywhere between 125 to 100 ka. This is followed by the deposition of flood plain fines that are bracketed between <97 ka and >70 ka. Broadly identified as the pluvial MIS-5a indicating condition nearly identical to that of the MIS-5e (Bradley, 1985). Following this the fluvial regime dwindled between 70 ka to 60 ka as indicated by the gritty sand horizon at Bahadarpur and medium to fine sand punctuated by sandy gravel channel bodies at Aritha (Fig. 3.5). This period represents a major transition from warm interstadial to cold stadial sub-stage when continental ice volume increased and the oxygen isotopic excursion in marine core show a shift towards heavier side This period is known as the drier MIS-4 (Bradely, 1985; Martinson et al., 1987; Lowe and Walker, 1997). Between <60 ka and 49 ka the fluvial regime reactivated in the basin. Since only lower part of the pedogenised silty sand horizon is preserved at Bahadarpur, and no upper age estimate for this horizon is available from Aritha, it can be inferred that the sedimentation could have started around <60 ka and continued > 25 ka (age of first fining upward sequence at Bahadarpur, Fig. 3.5). This period is identified as pluvial MIS-3 during which the global ice volume was reduced with relatively depleted oxygen isotopic signal in ocean records (Lowe and Walker, 1997) suggesting enhanced precipitation (Clemens et al., 1991). On land it is represented by large-scale fluvial aggradation in the river basins of Luni, Sabarmati and Mahi (Tandon et al., 1997; Juyal, et al., 2000; Srivastava et al., 2001; Kar et al., 2001).

Following this, a phase of climate instability is seen between 25 to 23 ka during which the basin experienced localized short-lived episodic events of fluvial activity.The widespread dry climate commenced during 21 ka, a period corresponding to global sea level lowering of around 120 m (Chappell, 1987) and global intensification of aeolian activity (Williams, 1975; Sarenthein, 1978). This period correspond to MIS-2.

Aeolian Sequences

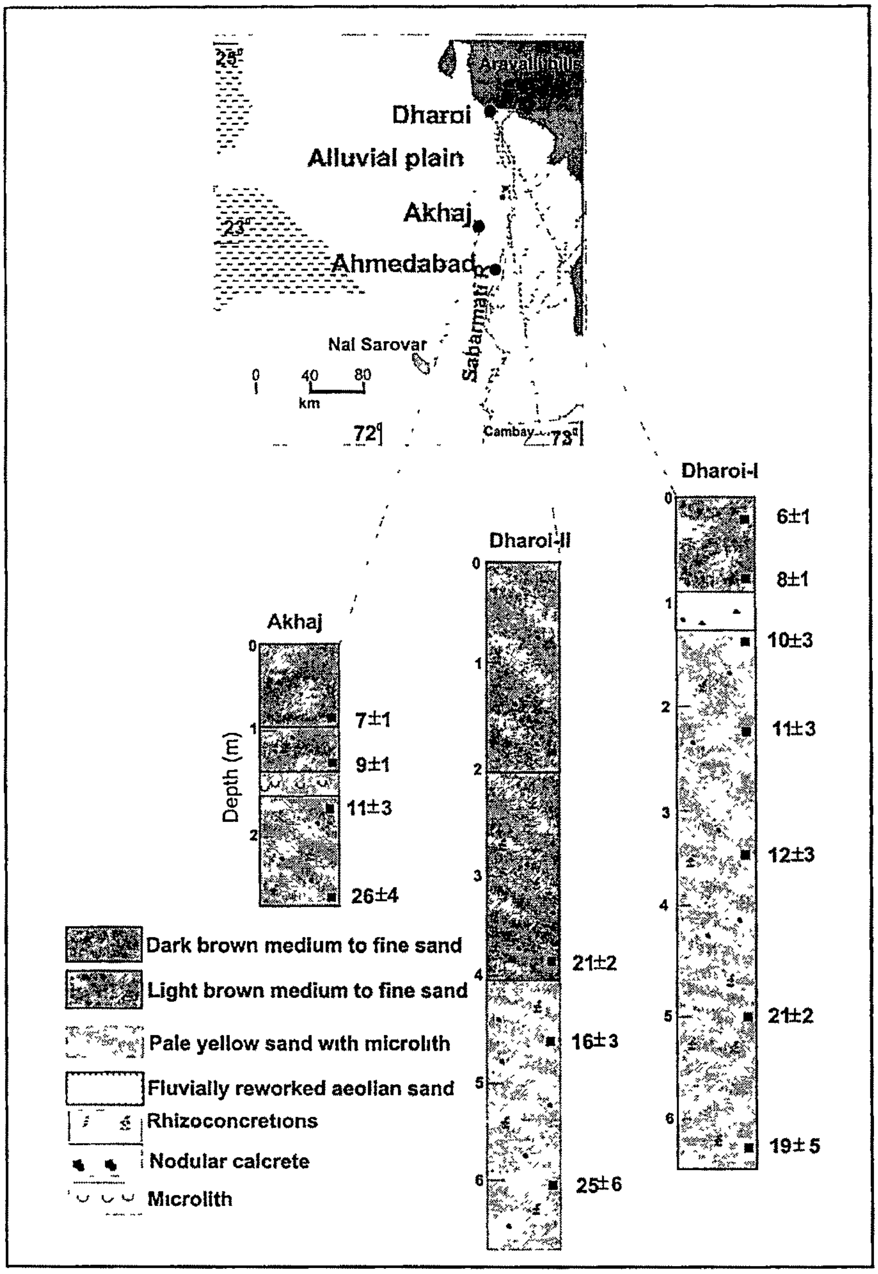

Figure-3.6. Chronology of aeolian sequences in the Sabarmati basin.

Dune chronology along the east west transects of the Thar desert has been reported by Chawla et al (1992); Thomas et al. (1999) and Kar et al. (2001). The present study deals with the dune records from the southern margin of the Thar, where extensive geoarchaeological and sedimentary records of climate change exist (Zeuner, 1952; Allchin and Goudie, 1971; Allchin et al., 1978) Preliminary data on the chronology of fossil dunes in the area is provided by Wasson et al. (1983); Tandon et al. (1997); Juyal et al. (2000) and Srivastava et al. (2001). In the study area, two types of dunes occur, (i) the poorly organized dunes (~ 3-6 m in height) and (ii) the obstacle dunes (~ 8-10 m in height) Close to the Little Rann of Kachchh, a small cluster of linear dunes has also been identified on satellite imagery (Wasson et al., 1983). In terms of their spatial distribution, poorly organized dunes occupy the upland terraces The obstacle dunes, on the other hand, cap the pediment surface of the Aravalli Hills

The detailed lithologs were prepared after trenching the dunes, aided by sedimentological analyses. Obstacle dunes are found in restricted localities abutting the Aravalli and Pavagarh hills. Two such localities viz. Dharoi (Sabarmati basin) and Tajpura (Mahi basin) were investigated in the present work. Poorly organized dunes are found all over the alluvial plain of Sabarmati, Mahi and Orsang basins. Basin wise description of the dunes stratigraphy is given below.

Sabarmati basin

Poorly organized dunes

(a) ***Akhaj:*** In a 3 m dune profile exposed along a road cutting near the village of Akhaj (Fig. 3.6) the upper 1.5 m was predominantly brown which graded to grey towards the bottom. Evidence of weak pedogenesis in the form of moderately developed ped faces, root casts and faint clay illuviation along the ped faces was seen. The layer between 1 5 m and 1.75 m contained microliths, charcoal pieces and bones, suggesting human occupation. Below this layer and upto 3 m depth, the sediments were less compact and light grey, containing 1-4 cm thick calcrete nodules

Obstacle dunes

(a) ***Dharoi-I:*** About 5 m thick section abutting the Aravalli hills was exposed along a seasonal rivulet west of the Dharoi dam. Dunes in this area occur in a narrow wind gap in the Aravalli hills (Fig 3 6) The upper 0 9 m of the profile comprised compact moderately pedogenized yellowish brown sand. This overlies 0.3 m thick fluvially reworked aeolian sand containing angular to sub-rounded pebbles of granite. At 1.2 m depth down to 5 m, the sand was pale yellow friable and contained carbonate concretions up to 10 cm thick.

(b) ***Dharoi-II:*** A 5.5 m thick section was exposed ~0.5 km west of Dharoi-1 (Fig. 3.6). The upper 2 m sequence comprised yellowish brown, compacted sand devoid of carbonate concretions. At 2 m to 4 m depth, the sand was grey to yellowish grey with 2-10 cm horizontally bedded carbonate concretions. Sediments at depth 4-6.5 m were yellowish grey with increasing carbonate concretions. Texturally, the sequence below 2 m depth is similar to Dharoi-I.

Mahi Basin

Poorly organized dunes

(a) ***Jaspur:*** In a 5 m thick dune section exposed on the left bank of Mahi River, two phases of dune accretion bisected by a fluvially reworked aeolian sand are seen (Fig. 3.7). Sequence begins with 2 m thick friable light grey sand having rhizoconcretions and nodular calcretes (~20 cm). This is overlain by moderately compact sand with occasional occurrence of nodular calcrete. This is overlain by 1 m thick moderately pedogenised light grey sand with nodular calcrete towards the upper part. Following this a 30 cm thick fluvially reworked sand occur. This is overlain by 1.5 m thick buff coloured moderately compact pedogenised sand that shows dispersed calcrete towards the upper part.

(a) ***Sultanpur:*** The dune section is 5 m thick and is located at the fringe of the older terrace at the left bank of Mahi River (Fig. 3.7). The lower 1.5 m is yellowish brown friable sand with dispersed nodular calcrete (~2cm) showing concentration towards the bottom. This is overlain by 3.5 m thick light yellow sand with irregularly dispersed friable calcretes. Their size increases towards the upper 1 m of the section.

(b) ***Dabka:*** A 4 m thick dune profile was exposed along the left bank of river Mahi near its estuary (Fig. 3.7). The yellow-brown aeolian sand rested unconformably on fluvio-aeolian sediment. The profile did not exhibit stratification except for the uneven distribution of 1-2 cm thick carbonate nodules

Obstacle dunes

(a) ***Tajpura-I:*** In a 4 m thick dune sequence located towards the southeastern face of the Pavagarh hill, the upper 1.6 m comprised moderately pedogenised, compact reddish light brown sand (Fig. 3.7). The horizon was devoid of carbonate concretions. Sediment from depth 1.6 m to 2.2 m was moderately compacted darker brown sand without carbonate nodules. From 2.2 to 3.7 m was pale yellow sand. Below 3 7 m, sediments were light grey with appearance of carbonate concretions. Allchin et al. (1978) reported Mesolithic artifacts on the surface and up to a few centimeters below the

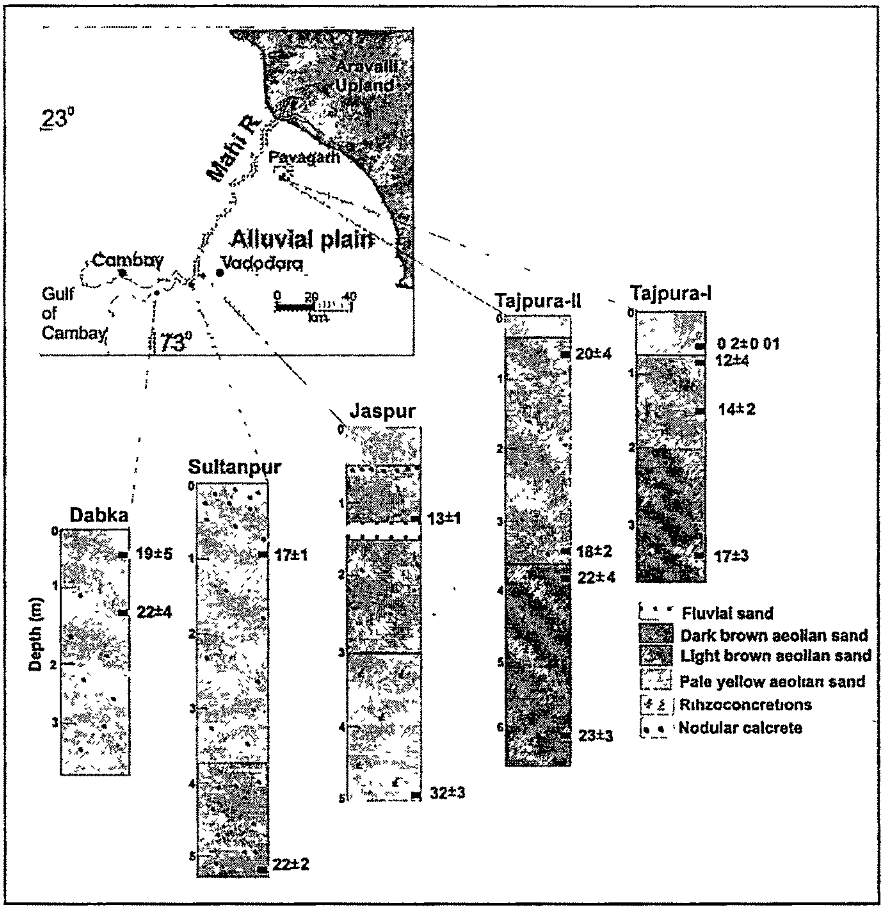

Figure-3.7. Stratigraphy and chronology of aeolian sequences in the Mahi basin.

dune crests

(c) ***Tajpura-II:*** A 6.5 m thick section was excavated 50 m west of Tajpura-I. The upper 3 5 m comprised moderately pedogenised, compact, reddish brown sand, broadly similar to Tajpura-I (Fig. 3.7). At depth 3.5 m to 6.5 m the sand is yellow to greyish yellow with increasing concentration of carbonate concretions and rhizoliths that were dispersed throughout.

Orsang basin

Poorly organized dunes in Orsang basin are relatively thin (2 to 3 m thick). They occur as sand sheet blanketing the fluvial sequence Two localities that are investigated along with the fluvial sequence are Bahadarpur and Aritha (Fig. 3.5). At these locations they are buff coloured, friable and contain dispersed nodular calcretes. The upper part of the horizon shows weak pedogenesis. It can be suggested that Orsang basin approximately limit the southern margin of fossil dunes in the region (Figs. 1.2 and 3.5).

Mean grain size of stabilized dunes varies between 2.1 to 3.7 ϕ (fine to very fine sand) and constitute 90to 99% of the sediment.

Chronology

Samples from freshly exposed dunes were collected in aluminium pipes. In general, several samples in a single profile at different depths were collected so as to assess the continuity/breaks in aeolian deposition. The experimental data and BGSL ages are shown in Table-3.6.

Dharoi-I

Sample No.	Depth (cm)	U(ppm)	Th(ppm)	K(%)	Dose Rate (Gy/ka)	ED(Gy)	Age (ka)
TR-249	20	2.0±0.4	7.0±1.5	1.28±0.1	2.2±0.2	12±3	6±1
TR-250	80	2.2±0.4	5.7±1.4	1.73±0.1	2.5±0.2	19±2	8±1
TR-252	130	1.0±0.4	5.9±1.5	1.19±0.1	1.8±0.2	18±5	10±3
TR-254	230	1.0±0.4	6.5±1.3	1.21±0.1	1.8±0.2	20±6	11±3
TR-255	350	1.6±0.3	2.8±0.1	1.27±0.1	1.8±0.1	22±5	12±3
TR-253	500	1.3±0.1	3.5±0.8	1.08±0.1	1.6±0.1	34±2	21±2
TR-256	620	1.4±0.5	9.0±1.6	1.38±0.1	2.3±0.2	42±10	19±5

Dharoi-II

Sample No.	Depth (cm)	U (ppm)	Th(ppm)	K(%)	Dose Rate (Gy/ka)	ED (Gy)	Age (ka)
TR-257	400	1.1±0.3	3.7±1.0	1.02±0.1	1.5±0.4	32±2	21±2
TR-258	450	1.0±0.3	3.7±1.0	0.80±0.1	1.3±0.1	21±4	16±3
TR-259	600	1.0±0.2	3.9±1.0	0.98±0.1	1.5±0.1	37±8	25±6

Akhaj

Sample No.	Depth (cm)	U (ppm)	Th(ppm)	K(%)	Dose Rate (Gy/ka)	ED (Gy)	Age (ka)
TR-243	50	1.1±0.4	6.3±1.5	0.4±0.02	1.2±0.2	8±0.2	7±1
TR-244	145	1.4±0.4	4.7±1.4	1.18±0.05	1.8±0.2	16±2	9±1
TR-246	180	1.1±0.3	3.5±1.0	0.85±0.04	1.3±0.1	22±5	11±3
TR-248	300	1.0±0.3	5.6±1.1	0.97±0.04	1.5±0.1	39±5	26±4

Tajpura-I

Sample No.	Depth (cm)	U (ppm)	Th(ppm)	K(%)	Dose Rate (Gy/ka)	ED (Gy)	Age (ka)
TR-233	70	1.3±0.4	5.6±1.4	1.60±0.10	2.2±0.2	0.4±0.2	0.20.01
TR-232	85	1.0±0.3	5.6±1.0	0.75±0.04	1.4±0.1	17±5	12±4
TR-229	160	1.3±0.2	3.4±0.7	0.60±0.03	1.2±0.1	16±2	14±2
TR-225	370	1.0±0.1	3.9±0.7	1.27±0.10	1.7±0.1	30±4	17±3

Tajpura-II

Sample No.	Depth (cm)	U (ppm)	Th(ppm)	K(%)	Dose Rate (Gy/ka)	ED (Gy)	Age (ka)
TR-260a	50	1.6±0.3	3.5±1.1	1.34±0.1	2.0±0.2	37±7	20±4
TR-260b	330	1.2±0.4	6.3±1.4	1.08±0.1	1.7±0.2	32±1	18±2
TR-261	390	1.0±0.3	5.3±1.0	1.04±0.1	1.6±0.1	75±19	46±12
TR-262	390	1.0±0.2	4.0±1.0	1.08±0.1	1.5±0.1	34±6	22±4
TR-263	600	0.6±0.2	6.0±1.0	1.18±0.1	1.7±0.1	39±3	23±3

Dabka

Sample No.	Depth (cm)	U (ppm)	Th(ppm)	K(%)	Dose Rate (Gy/ka)	ED (Gy)	Age (ka)
TR-242	60	1.5±0.5	8.0±1.6	1.17±0.1	2.0±0.2	38±9	19±5
TR-241	150	2.1±0.5	6.3±1.7	1.14±0.1	2.0±0.2	44±6	22±4

Jaspur

Sample No.	Depth (cm)	U (ppm)	Th(ppm)	K(%)	Dose Rate (Gy/ka)	ED (Gy)	Age (ka)
DJ-3	125	2.3±0.4	9.2±1.4	1.10±0.05	2.2±0.2	29±1	13±1
DJ-1	500	2.0±0.4	7.1±1.5	1.04±0.05	2.0±0.2	63±1	32±3

Sultanpur

Sample No.	Depth (cm)	U (ppm)	Th(ppm)	K(%)	Dose Rate (Gy/ka)	ED (Gy)	Age (ka)
MSD-4	100	1.4±0.2	3.7±1.0	1.12±0.05	1.7±0.1	29±1	17±1
MSD-1	540	2.0±0.5	6.8±1.6	1.16±0.06	2.0±0.2	45±1	22±2

Cosmic ray dose 150µ Gy/a, Water content taken 10±5%

Table 3.6 Experimental data and BGSL ages obtained on aeolian sequences.

Figures 3.5, 3.6 and 3.7 show the aeolian stratigraphy, along with the BGSL ages obtained from Sabarmati, Mahi and Orsang basins. The ages range from 32±3 to 6±1 ka. A lone exception is an age of 0.2 ka (TR-233, Table-3.6) that perhaps reflects a recent human activity and consequently has not been considered. Broadly, the chronology suggests that dune accretion in the region pre-dates the Last Glacial Maximum (LGM) placed at [21,648 (21,484) 21,313] cal a BP (Porter, 2001) and that the final phase of dune deposition occurred during the Mid-Holocene. Thicker obstacle dunes preserve amplified record of dune deposition compared to the poorly organized dunes. BGSL ages enable the following deductions:

(i) In the Sabarmati (Akhaj) and the Mahi (Jaspur) basins, the luminescence ages

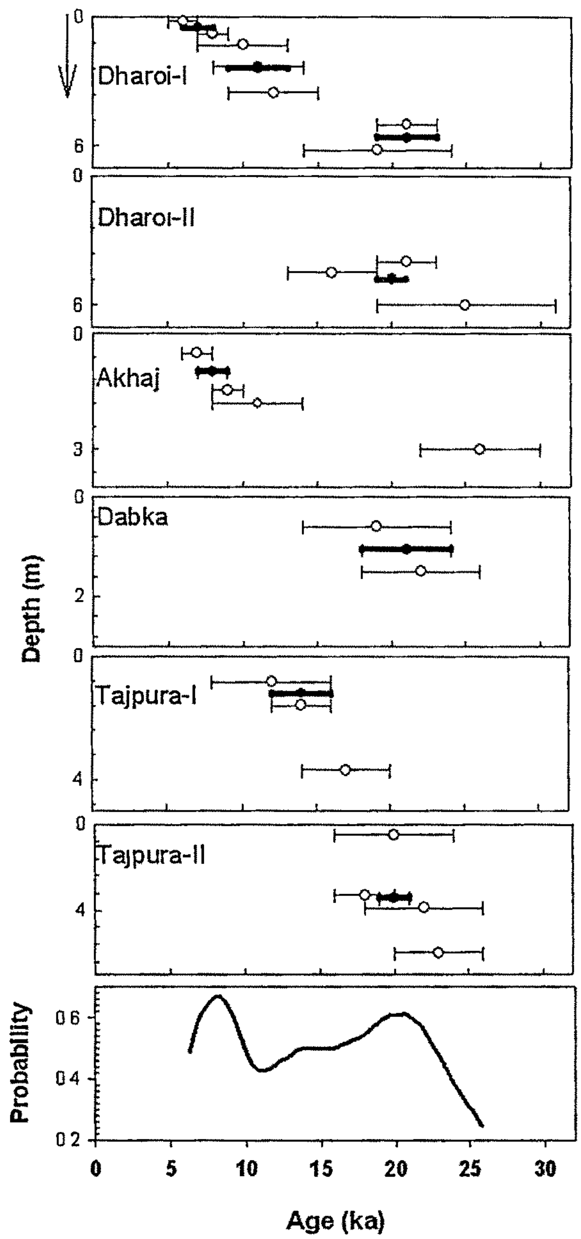

Figure-3.8. BGSL ages plotted against depth, shown with open circles along with error bars. Arrow at left indicates from surface towards the bottom. Weighted mean of ages along with error bars is shown with thick black lines and filled circles. The bottom most box shows the probability distribution of ages clustering around 24 – 18 ka and 9 – 6 ka

indicate dune deposition during 26±4 ka and 32±3 ka, respectively.

(ii) The termination in the dune deposition, however, occurred at different times i.e. 11±1 ka in Mahi basin and 6±1 ka in Sabarmati basin (Table-3.6, Figs 3.6 and 3.7).

(iii) During the period between 12±4 to 8 ±1 ka, aeolian deposition was subdued. This was climate-controlled, as reflected by the presence of microlith between 11±3 ka and 9±1 ka, and fluvially reworked aeolian sand between 10±3 ka to 8±1 ka (Fig. 3.6).

(iv) Near Mahi estuary at Dabka and Sultanpur (Fig. 3.7), the upper part of the dune sections were dated to 19±5 ka and 17 ±1 ka, respectively. Absence of younger sand implies that it should have been deflated and transported inland.

(v) The error-weighted mean ages, when plotted *vs*. depth (Fig. 3.8), show two events of dune accretion around 24-18 ka and 9-6 ka. However, error-corrected probability density distribution plots (Venkatesan and Ramesh, 1993) also indicate a weak cluster between 17 to 12 ka, in addition to the above clusters.